IRIS AperTO

UNIVERSITÀ DEGLI STUDI DI TORINO

AperTO - Archivio Istituzionale Open Access dell'Università di Torino

An inhibitory antibody targeting Carbonic Anhydrase XII abrogates chemoresistance and significantly reduces lung metastases in an orthotopic breast cancer model in vivo

This is a pre print version of the following article:

Original Citation:

Availability:

This version is available http://hdl.handle.net/2318/1670022 since 2018-10-04T15:47:01Z

Published version:

DOI:10.1002/ijc.31607

Terms of use:

Open Access

Anyone can freely access the full text of works made available as "Open Access". Works made available under a Creative Commons license can be used according to the terms and conditions of said license. Use of all other works requires consent of the right holder (author or publisher) if not exempted from copyright protection by the applicable law.

(Article begins on next page)

05 May 2023

An inhibitory antibody targeting Carbonic Anhydrase XII abrogates chemoresistance and significantly reduces lung metastases in vivo

Bettina von Neubeck[1*], Gabor Gondi[1*], Chiara Riganti[2], Chenchen Pan[3], Arnaldo Parra Damas[3], Hagen Scherb[4], Ali Ertürk[3] and Reinhard Zeidler[1, 5]

[1] Department of Gene Vectors, Helmholtz Center for Environmental Health, Munich, Germany; [2] Department of Oncology, University of Torino, Italy; [3] Institute for Stroke and Dementia Research, Klinikum der Universität München, [4] Institute of Computational Biology (ICB), Helmholtz Center for Environmental Health, Munich, Germany, [5] Department of Otorhinolaryngology, Klinikum der Universität München, Munich, Germany.

* Both authors contributed equally to this work

Correspondence to:

Reinhard Zeidler, Ph. D.
c/o Helmholtz Center
Marchioninistr. 25
81377 Munich / Germany
Tel: ++4989-31871239
Email: Reinhard.Zeidler@med.lmu.de

Keywords: CAXII, triple-negative breast cancer, 6A10 antibody, chemoresistance, P-glycoprotein

Abstract

Carbonic Anhydrase XII (CAXII) is a membrane-tethered ectoenzyme involved in intracellular pH regulation and overexpressed across various types of human cancer. Because CAXII inhibition shows antitumor activity *in vitro*, it is thought that the enzyme is mandatory for maximum tumor growth, above all under hypoxic conditions. Recently, it has been shown that CAXII is co-expressed along with the P-glycoprotein (P-GP) on many tumor cells and that both proteins physically interact. Of interest, blocking CAXII activity also decreases P-GP activity in cancer cells both *in vitro* and *in vivo*.

Previously, we have reported on the development of a monoclonal antibody, termed 6A10, which specifically and efficiently blocks human CAXII activity. Here we demonstrate that 6A10 also indirectly reduces P-GP activity in CAXII/P-GP double-positive chemoresistant cancer cells, resulting in enhanced chemosensitivity as revealed by enhanced accumulation of anthracyclines and increased cell death *in vitro*. Even more important, we show that mice carrying human triple-negative breast cancer xenografts co-treated with doxorubicin (DOX) and 6A10 show a significantly reduced number of metastases.

Collectively, our data provide evidence that the inhibition of CAXII with 6A10 is an attractive way to reduce chemoresistance of cancer cells and to interfere with the metastatic process in a clinical setting.

Introduction

Breast cancer (BC) is one of the most common types of cancer in women and the most frequent cancer-associated cause of death. Whereas patients with still localized tumors have an excellent clinical prognosis, it is dramatically worse in patients with disseminated cancer, consistent with the fact that distant metastases are by far the most frequent cause of cancer-related death. As with many types of cancer, therapeutic effectiveness in BC is often limited by intrinsic or acquired multidrug resistance (MDR) of tumor cells against chemotherapeutic agents. MDR is frequently a direct consequence of treatment (1) and is characterized by the overexpression of members of the ATP Binding Cassette (ABC) transporter family, which actively extrude various cytotoxic drugs out of cancer cells. The best investigated MDR protein is P-glycoprotein (P-GP), also referred to as MDR1 or ABCB1 (2). Due to its central role in multidrug-resistant cancer cells, direct inhibition of P-GP has been regarded as an attractive approach to reduce MDR, but the clinical application of direct P-GP inhibitors has been limited by serious adverse effects and most of these drugs have failed to improve therapeutic efficacy (3).

The carbonic anhydrases (CAs) constitute a family of ubiquitous zinc metalloenzymes, which all catalyze the reversible hydratation of CO_2 to carbonic acid, which rapidly decomposes into bicarbonate and protons (4). The production of bicarbonate is necessary for a variety of physiological processes including respiration and pH homeostasis (5). CAXII, alongside with CAIX, is a membrane-tethered ectoenzyme, which is highly overexpressed across many types of cancer, including BC (6, 7). CAXII contributes to intracellular pH regulation, which is of particular relevance to metabolically active hypoxic tumor cells to cope with an acidic tumor environment (8). Consequently, its inhibition shows – to some extent – anti-proliferative effects both *in vitro* and *in vivo* (9–13). Our group developed the first CAXII-inhibitory antibody (6A10), which led to reduction of tumor cell growth *in vitro*. In addition, 6A10 also revealed anti-tumor activity in a xenograft lung carcinoma model where the antibody led to a significant reduction of tumor load and increased overall survival (14, 15).

Of note, it has been demonstrated recently that CAXII physically interacts with, and regulates the activity of, P-GP and in chemoresistant cancer cells. In addition, a genetic CAXII knock-down in P-GP-positive cancer cell lines resulted in enhanced chemosensitivity (16). We show here that the blocking CAXII-specific monoclonal antibody 6A10 interferes with P-GP activity in chemoresistant cancer cell lines, thus increasing the sensitivity against clinically relevant anthracyclines. Even more important, we demonstrate in a human xenograft breast cancer model that the co-treatment with doxorubicin (DOX), a substrate of P-GP, and 6A10 significantly reduces metastases of chemoresistant cells to the thorax.

Results

6A10 reduces P-GP activity in chemoresistant CAXII^{high}/P-GP^{high} breast cancer cell lines *in vitro*

It has been demonstrated recently that CAXII and P-GP are co-expressed in many chemoresistant human cancers, that CAXII activity is relevant for the chemoresistant phenotype of these cells, and that a silencing of CAXII with siRNAs restores chemosensitivity (16). Because this type of intervention is not possible *in vivo*, we investigated whether the CAXII-inhibitory antibody 6A10 also interferes with P-GP-mediated chemoresistance.

To this end, we first defined the expression levels for CAXII (Figure 1A) and P-GP (Figure 1B) in a panel of human breast cancer cell lines. To assess the chemosensitizing effect of 6A10, we first incubated P-GP^{high}/CAXII^{high} MDA-MB-231 cells in the presence of 6A10 and the anthracyline doxorubicin (DOX), which is a P-GP substrate and is regularly used as a chemotherapeutic agent in breast cancer patients. After 24 hours, we measured the intracellular DOX accumulation and the LDH release, which are markers for P-GP activity and DOX-cytotoxicity, respectively. 6A10 had a dramatic effect in DOX-treated P-GP^{high}/CAXII^{high} MDA-MB-231 cells, in which the co-incubation with DOX and the 6A10 antibody resulted in significantly elevated intracellular DOX concentrations (Figure 1C) and cytotoxicity (Figure 1D). In line, co-incubation with DOX and 6A10 also led to a significant reduction in P-GP activity (Figure 1E). We obtained similar results in P-GP^{high}/CAXII^{high} chemoresistant human cancer cell lines derived from colon, lung and bone (Figure S1), showing that this effect is not restricted on breast cancer cells, only.

In contrast, the co-incubation with 6A10 and DOX had no detectable additive or synergistic effect onto intracellular DOX accumulation or cytotoxicity on P-GP$^{low/-}$ or CAXII$^{low/-}$ cell lines MCF7, SkBr3 and T47D (Figure 1F and 1G)

Taken together, our data demonstrate that CAXII regulates P-GP activity in cancer cells and that the CAXII-specific blocking antibody 6A10 increases the chemosensitivity of P-GP-positive chemoresistant cancer cells, resulting in increased intracellular DOX accumulation

and subsequent cell death. Similar results were observed with daunorubicin (DAU), another clinically relevant anthracycline (Figure S2).

Knocking-down CAXII or P-GP abrogates the chemosensitizing effect of 6A10

To corroborate the specificity of the effects observed in the previous set of experiments, we first knocked-down P-GP in MDA-MB-231 cells by transfecting cells with two different siRNAs specific for P-GP. As a control, cells were treated with a scrambled siRNA. An immunoblot on lysates from siRNA-treated cells collected two days after transfection revealed almost complete P-GP depletion (Figure 2A) and an almost complete reduction of P-GP activity in contrast to cells treated with a scrambled control siRNA (Figure 2B). We next treated these cells with DOX and 6A10 as described above. As shown, the siRNA-mediated knock-down of P-GP resulted in elevated sensitivity against DOX as substantiated by increased intracellular DOX accumulation (Figure 2C) and LDH release (Figure 2D). However, 6A10 treatment had no additional effect in the P-GP knock-down cells while retaining activity in MDA-MB-231 cells treated with the control siRNA.

To unambiguously proof that CAXII directly regulates P-GP activity, we next generated two CAXII knockout MDA-MB-231 clones using CRISPR-Cas9 technology and controlled the complete CAXII knockout by flow cytometry (Figure 2E). As observed with the P-GP knock-down cells, the CAXII knockout resulted in a significantly decreased P-GP activity, albeit to a lesser extent (Figure 2F). Functional assays revealed that the CAXII knockout cells were much more sensitive against DOX than parental cells and that 6A10 – as expected – revealed no additional chemosensitizing effect (Figures 2G and 2H). Again, similar results were also obtained with DAU (Figure S3).

Thus, we conclude that CAXII directly regulates P-GP activity in MDA-MB-231 cells, and that 6A10 has a CAXII-dependent robust chemosensitizing effect.

6A10 has no effect onto established bulky tumors in DOX-treated tumor bearing NSG mice

Having shown that blocking CAXII with the 6A10 antibody impairs P-GP activity in P-GP^{high}/CAXII^{high} cells and, in parallel, increases their sensitivity against anthracyclines, we decided to investigate the effect of 6A10 onto tumor growth and metastases formation in an orthotopic xenograft model. For this model, we used chemoresistant MDA-MB-231 cells that have been demonstrated recently to recapitulate the whole metastatic process in NSG mice, develop metastases in distant organs (17) and respond to 6A10 treatment *in vitro*. We used MDA-MB-231/mCherry/LUC cells that were obtained by transducing MDA-MB-231 cells with a lentiviral vector encoding firefly luciferase (LUC) and mCherry (18) in order to follow tumor growth and dissemination by bioluminescence imaging (BLI) and to assess tumor spread in whole-organs using tissue clearing and fluorescent light-sheet microscopy imaging, respectively.

In a first series of experiments, we injected different numbers of MDA-MB-231/mCherry/LUC cells ranging from 5 x 10^4 to 2 x 10^6 cells into NSG mice and performed BLI two weeks later. This experiment revealed that 2 x 10^6 cells inoculated orthotopically into the mammary fat pad was the minimum cell number that gave rise to tumors in 100% of the animal (data not shown). In parallel, we tested the activity of different concentrations of DOX onto the growth of the injected MDA-MB-231/mCherry/LUC cells as well as for systemic adverse effects. This investigation revealed that DOX at a concentration of 2 µg/g of body weight slightly delayed tumor growth without eradicating it completely while not showing significant systemic toxicity (data not shown). Thus, for the main experiment, 2 x 10^6 MDA-MB-231/mCherry/LUC were orthotopically injected per mouse and tumor growth was followed by BLI as described (15). Two weeks after injection, tumors had reached a size detectable by BLI and animals were randomized into five different groups (n=8 per group).

From then on, mice were treated intravenously with 6A10 or an isotype control antibody at a concentration of 100 µg/mouse twice per week and/or with DOX at a concentration of 2 µg/g of bodyweight twice per week. During this period tumor growth and dissemination was

followed by BLI once a week until the experiment had to be terminated at nine weeks post injection for reasons of welfare of mice from the untreated group. As shown in the box plot in Figure 3A, neither DOX nor 6A10 treatment, alone or in combination, revealed an inhibitory effect onto the growth of the primary tumor judged by the total BLI signal.

6A10 significantly reduces the number of metastases in DOX-treated tumor bearing NSG mice

As demonstrated recently in NSG mice, orthotopically implanted MDA-MB-231 human BC cells frequently migrate to axillary lymph nodes and to the lungs where they consistently form macro-metastases (17). Despite the fact that the overall BLI signals did not differ significantly among groups, we scrutinized the BLI signals obtained only from the thorax in more detail. This analysis revealed that co-treatment of tumor-bearing animals with DOX and 6A10 significantly decreased the tumor burden in the thorax (Figure 3B). In detail, six out of eight animals had no detectable thorax signal and only two animals developed visible metastases. One animal developed a small tumor mass probably in an axillary lymph node with no detectable signal in the lungs. Only one animal of the co-treatment group revealed an extensive thoracic BLI signal at week nine post injection (Firgue 3C). In contrast, most of the mice of the other groups had clear thoracic BLI signals indicative for lung and lymph node metastases (Figure 4). Of note, neither treatment with DOX alone or 6A10 alone revealed a significant inhibitory effect onto the development of metastases.

A thorough statistical analysis revealed that co-treatment with DOX and 6A10 significantly reduced the number of thorax metastases over time as compared to animals treated with DOX only ($p=0.005$) or compared to animals left completely untreated ($p<0.0001$) (Figure 3C and 3D). 6A10 used as a monotherapy had no significant therapeutic effect compared to untreated animals ($p=0.7$). This result is thus in line with *in vitro* data described above and by others (16) demonstrating that CAXII inhibition chemosensitizes P-GP^{high}/CAXII^{high} tumor cells.

Whole-organ imaging confirms the reduction of metastases by combinatorial treatment with DOX and 6A10

Next, we analyzed the metastatic process at the cellular level in whole organs. To this end, we performed optical tissue clearing of intact lungs and imaged the mCherry expressing tumor cells in transparent lungs by light-sheet microscopy (19). Then, we quantified the tumor load in an unbiased manner in the complete lungs, where the major metastases have been expected. 3D reconstructions and quantifications of cleared lungs confirmed the above findings: The number and the volumes of tumors in DOX + 6A10 co-treated mice were significantly reduced as compared to untreated and DOX treated mice (Figure 4). In contrast, DOX alone neither had significantly fewer micrometastases nor smaller volumes as compared to untreated animals ($p=0.2$ and $p=0.2$, respectively).

These data suggest that while DOX treatment alone reduced the volume of micrometastases but could not eliminate them *in toto*, treatment of DOX and 6A10 together eradicated almost all micrometastases including the small volumes.

Discussion

MDR of cancer cells is a major clinical obstacle that often limits the success of treatment. Consequently, interfering with chemoresistance is regarded as an attractive approach to increase the efficacy of chemotherapies. While bulky solid tumors can normally be removed surgically, the treatment of resistant residual cells or single invading cells is much more challenging and still remains a major problem to overcome. Given that most cancer patients die from distant metastases, treatment strategies aiming at reducing the invasion process of these resistant cells and the formation of metastases at distant sites and organs are crucial for an improvement of cancer treatment (20). However, despite intensive research on small molecule inhibitors of P-GP, one of the main protein mediating MDR, all compounds so far showed severe side effects and, therefore, could not be used in the clinics (21, 22).

here, we show that it is possible to overcome chemoresistance with the CAXII-blocking antibody 6A10. Although 6A10 does not target P-GP directly, it has a tremendous effect on P-GP activity *in vitro*, resulting in an increased intracellular accumulation of DOX and, consequently, to increased cellular cytotoxicity. The molecular mode of action of how 6A10 interferes with P-GP activity is not fully understood, but given that both proteins interact physically, it is tempting to speculate that CAXII inhibition locally perturbs intracellular pH regulation and thus P-GP activity. Indeed, the optimal pH at which P-GP works is around 7.6; transiently CAXII inhibition and/or pharmacological inhibition with the broad-spectrum CA inhibitor acetazolamide lowers the pH at 7.4, decreasing P-GP activity by about 25% (16).

To investigate the relevance of CAXII-mediated chemosensitization in the *in vivo*-situation, we performed an orthotopic breast cancer model, in which co-treatment with DOX and 6A10 did not show any additive or synergistic effect onto the primary tumors. This result didn't come to our surprise, as monoclonal antibodies are known to have only limited effects onto bulky solid tumors due to e.g. poor tissue penetration (23, 24). In our xenograft model, we used triple negative MDA-MB-231 breast cancer cells, which are known to grow aggressively in immunocompromised hosts and to metastasize to different organs, above all the lungs

(17). Therefore, we were much more interested whether DOX + 6A10 co-treatment has an inhibitory fact on the metastasizing cells.

Even though DOX and 6A10 co-treatment had no growth-inhibitory effect on the primary tumors, co-treated animals revealed significantly lower numbers of metastases to the thorax as compared to animals treated with DOX or 6A10 alone. We could demonstrate that it is possible to target invading single tumor cells and micrometastases and sensitize these resistant tumor cells to chemotherapy without increasing systemic toxic side effects. Thereby the prevention of the so called metastatic colonization (20) of a single cell and the outgrowth of macrometastases at a distant site may hold the most therapeutic promise using 6A10 in the adjuvant setting and can constitute a new therapeutic approach to treat invasive chemoresistent metastatic cancers.

We were able to further specify these results by analysis of metastases in the lungs at the single cell level using a recently developed method of tissue clearing and whole-organ imaging by light-sheet microscopy (19, 25, 26). The quantification of metastases showed that treatment with DOX led to smaller metastases, compared to untreated animals. In contrast, the combinatorial treatment of DOX and 6A10 completely eradicated all metastases in the lungs of almost all co-treated animals.

Besides preventing metastasis, relapse originating from outgrowing disseminated tumor cells after surgical removal of the main tumor due to residual single resistant cells could also be prevented by the combinational therapy of 6A10 and anthracyclines. In addition to interference with chemoresistance, treatment with 6A10 might also activate antitumoral immune responses like complement-dependent cytotoxicity (CDC) or antibody-depended cell-mediated cytotoxicity (ADCC), thus targeting immune cells specifically to invading tumor cells.

In conclusion, we demonstrate that the CAXII blockade by 6A10 antibody significantly reduces P-GP activity, which represents a novel therapeutic approach to improve the treatment of metastatic and chemoresistant cancers. Further investigations are necessary to

analyze the molecular mechanisms behind the interaction of P-GP mediated MDR and CAXII.

Materials and Methods

Cells and culture conditions

Cell lines were kindly provided by Dr. Chiara Riganti, Department of Oncology, University of Torino, Italy. Identity of the MDA-MB-231 cells, which were used for the *in vivo* experiments, was verified by ST-PCR (Eurofins, Ebersberg, Germany). All cell lines were cultured in RPMI 1640 medium supplemented with 8% v/v fetal bovine serum, 1% v/v L-Glutamine and 1% v/v penicillin-streptomycin. Chemoresistant cell lines HT29/DX, A549/DX and U2OS/DX were generated out of the parental cell lines as previously described (27).

Flow Cytometry

For flow cytometric analysis of CAXII expression, cells were stained with 1 µg of 6A10 in FACS-Buffer (PBS + 2% FCS) for 20 min followed by staining with an anti-rat-Alexa Fluor® 488 secondary antibody (Abcam).

Western blotting analysis

For analysis of P-GP expression by western blotting, whole cell lysates were prepared as previously described (27). 60 µg of cell lysate was used for SDS-PAGE and P-GP was detected by an anti-P-GP antibody (mouse C219; Millipore), followed by a peroxidase-conjugated secondary antibody. An anti-β-tubulin antibody served as an internal control (rabbit, Abcam).

Pgp and CAXII knockout

CAXII knockout clones were established by transfection of MDA-MB-231 cells with 1 µg of CAXII CRISPR guide RNA vector plus 1 µg of vector coding for puromycin resistance using Metafectene® Pro (Biontex), following the manufacturer's instructions. After 16 hours selection with puromycin started and single cell clones were established. The stable knockout of CAXII in each single clone was validated by analysis of CAXII expression by flow cytometry using 6A10 as a primary antibody.

PG-P silencing was performed as previously described (16). Basically, cells were transfected with control scrambled siRNA or specific siRNAs for P-GP (Santa Cruz Biotechnology).

Knock down of P-GP expression levels were verified by qRT-PCR (data not shown) and western blot.

Analysis of intracellular drug accumulation

The anthracyclines DOX and DAU can be quantified by fluorimetric analysis at excitation 485 nm and emission 553 nm. To analyze the intracellular drug accumulation, cells were seeded in 6-well plates until 70% of confluence was reached and medium was supplemented with 5 µM DOX or 5 µM DAU. If P-GP inhibitor Verapamil (75 µM) or 6A10 (20 µg/ml) were used in combination with anthracyclines, cells were pre-incubated for 20 min before addition of anthracyclines. Intracellular drug accumulation was measured 24 h later. Therefore, cells were harvested and pelleted. The cell pellet was re-suspended in ethanol/HCl 0,3 N (1:1 v/v), sonicated (one burst, 10 sec, 40% power) and the protein content was determined using a Pierce™ BCA Protein Assay Kit. To measure the content of DOX and DAU, 25 µl of each sample was loaded in a black walled 96-well plate and measured fluorimetrically. The concentration of each drug was determined by a titration curve and normalized on the protein content of each sample.

Cytotoxicity Assay (LDH-Assay)

Cytotoxicity of the anthracyclines DOX and DAU in combination with 6A10 was analyzed by measuring the extracellular and intracellular LDH-activity of culture supernatant and cells, respectively, after incubation with drugs. The cytotoxicity was analyzed by the ratio of extracellular LDH-activity versus intracellular LDH-activity. LDH-activity was determined by the spectrophotometric analysis of NADH consumption at 340 nm over time.

Cells were incubated in a 6-well plate until 70% confluence and treated as described above. After an incubation time of 24 h, cell culture supernatant was collected for the analysis of extracellular LDH-activity and centrifuged at 14,000x g for 30 sec. To analyze the intracellular LDH-activity, cells were harvested, re-suspended in TRAP-Buffer (300 mM triethanolamine, pH 7.6) and sonicated (one burst, 10 sec, 40% power). The protein content was determined by using the Pierce™ BCA Protein Assay Kit. 50 µl of cell culture supernatant and 5 µl of cell lysate were supplemented with 250 µl reaction buffer (0.3 mM NADH/0.6 mM pyruvic acid,

solved in TRAP-buffer) and incubated for 6 min at 37 °C in a plate reader. During that time, the absorbance change at 340 nm was measured every 30 sec.

The reaction kinetics of NADH oxidation was analyzed using the Lambert-Beer law and the molar attenuation coefficient ε of NADH (9.31 dAbs/µmol/min). All values were normalized on the used amount of protein and displayed as the ratio of extracellular LDH-activity to total LDH-activity (extracellular plus intracellular LDH-activity).

P-GP ATPase activity assay

The analysis of P-GP Activity was performed on isolated membrane fractions from MDA-MB-231 cells as previously described (28). The enzymatic activity was measured by quantification of free phosphate (Pi) released by ATPase activity of P-GP. Briefly, cells were incubated in a 10-cm cell culture dish and grown until 70% of confluence was reached. Medium was replaced with 5 ml of medium supplemented with either 20 µg/ml of 6A10 or 100 µM Verapamil. Cells incubated without additives served as a control. After 1 h of incubation membrane fractions were isolated according to (16). The protein content of each sample was determined by BCA protein assay (Pierce^{TM} BCA Protein Assay Kit).

For analysis of P-GP ATPase activity, 50 µl of each sample was supplemented with 50 µl of reaction buffer (25 mM Tris/HCl, 50 mM KCl, 2.5 mM $MgSO_4$, 0.5 mM EGTA, 3 mM ATP, 3 mM DTT, 2 mM ouabain, 3 mM NaN_3, pH 7.4) and transferred to a 96-well plate, followed by an incubation at 37°C for 30 min. In each experiment, 0.5 mM Na_3VO_4 was used as a blank. To stop the reaction, 200 µl cold stopping buffer (0.2% ammonium molybdate (w/v), 1.3% H_2SO_4 (v/v), 0.9% SDS (w/v), 2.3% trichloroacetic acid (w/v), 1% ascorbic acid (w/v)) were added and incubated at RT for 30 min. The absorbance was measured at 620 nm followed by the quantification of the amount of released Pi by using a titration curve previously prepared and normalized on the amount of protein used for each reaction. The enzymatic activity was displayed as percentage of ATPase activity of the control sample of untreated cells.

Animals and Orthotopic breast cancer model

Female NSG mice (NOD-scid IL2Rγ$^{-/-}$) were obtained from Charles River Laboratories (Munich, Germany) and housed at the animal facility of the Helmholtz Center Munich under 12 h light/dark cycles with food and drinking provided *ad libitum*. All experiments were carried out under a license from the State of Bavaria.

MDA-MB-231 cells were transduced with a bicistronic lentivirus encoding mCherry and enhanced firefly luciferase (29). Cells expressing the highest CAXII and mCherry levels were sorted using a Becton Dickinson Aria III cell sorter to yield a homogenous cell population. 2 x 10^6 MDA-MB-231/mCherry/fLUC cells were re-suspended in 50 µl RPMI without additives and injected into the left inguinal mammary fad pad. Tumor growth was followed twice a week for two weeks by bioluminescence imaging. Therefore, mice were injected with luciferin (150 mg/kg *i.p.*), anesthetized with isoflurane, and bioluminescence signal was measured 15 min after injection using an IVIS II Lumina Imaging system (Caliper Life Science, Mainz, Germany). The bioluminescence signals were quantified with the Living Image software (Caliper) and displayed in photons/sec.

Two weeks after cell injection all mice developed a solid tumor at the injection site. Mice were randomly distributed into 5 groups each consisting of 8 animals and treatment started twice a week intravenously with 2 µg/g body weight DOX, 100 µg 6A10 or isotype control antibody or left untreated. Tumor signals were continuously measured once a week by bioluminescence imaging for 8 weeks after treatment has started.

Whole-body clearing and imaging of transparent intact lungs

Intracardial perfusion of mice was performed as previously described (Pan et al., 2016 Nat. Methods). In short, the mice were anesthetized with a combination of midazolam, medetomidine and fentanyl (MFF) before intracardial perfusion with 0.1 M PBS + heparin (10 U/ml) at 100-125 mm Hg pressure until blood was washed out, followed by 4% paraformaldehyde (PFA) in 0.1 M PBS for 10-20 min. Afterwards, the skin was carefully removed and the bodies were post-fixed in 4% paraformaldehyde for 1 day at 4 °C and stored in 0.1 M PBS (if needed). Subsequently, the whole-body DISCO clearing of fixed mice, consists of two major steps were performed: dehydration step with the serial gradient

alcohols and refractive index matching in the organic solvents (19). Cleared mouse lungs were imaged with the light-sheet microscopy as we described previously in detail (19, 26).

Statistical Analysis

For the comparison of the tumor development over time in the thorax during 8 weeks of treatment, the time trends of the log photons per sec were analyzed using SAS/STAT software 9.4 procedures GLM and MIXED for repeated measure analyses (SAS Institute Inc: SAS/STAT software User's Guide, Version 9.4, Cary NC: SAS Institute Inc., 2013). Assessing the time trends and possible trend differences of the log photons per sec between treatment groups requires consideration of the between-group effects as well as the within-subject effects. Typically, control and exposed groups start off with approximately equal counts but may be different in their average counts by the end of the study period. Therefore, the changes in the counts of the log photons per sec were quantified and tested by appropriate group∗time interaction parameter estimates with 95%-confidence intervals and corresponding p-values for the null hypotheses of no trend differences. The t-Test was employed for the comparison of mean values. The global level of significance was chosen to be 0.05. Results were considered significant when the p-value was smaller than 0.05. In case of small samples or skewed distributions, e.g. due to outliers, the exact Wilcoxon two-sample test (SAS procedure NPAR1WAY) was used.

Figures and Figure Legends

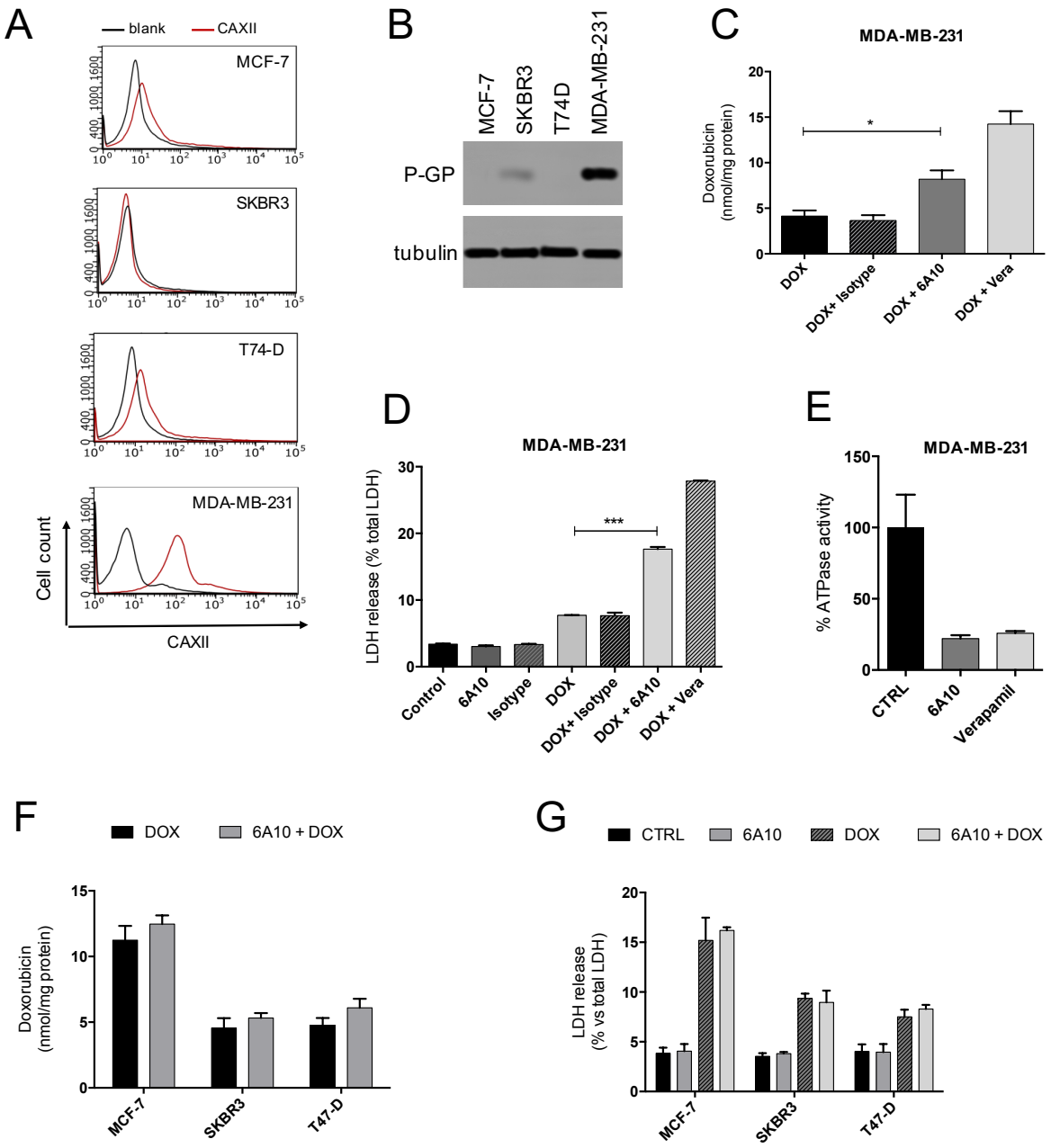

Figure 1

Figure 1: 6A10 increases intracellular accumulation of anthracycline doxorubicin (DOX) as well as cytotoxicity on CAXII^{high}/P-GP^{high} chemoresistant triple negative MDA-MB-231 breast cancer cells and directly impairs function of MDR-transporter P-GP. (A) Flow cytometric analysis of CAXII expression of different breast cancer cell lines. Stainings were performed with 6A10 as primary antibody. Blank: Isotype control antibody. (B) Western Blot Analysis of P-GP expression. β-Tubulin was used as a control for equal protein loading. (C) Analysis of intracellular DOX accumulation in CAXII^{high}/P-GP^{high} chemoresistant MDA-

MB-231 breast cancer cells. Cells were treated with 5 µM of DOX in combination with 20 µg/ml 6A10 antibody, an isotype control antibody or 75 µM P-GP inhibitor Verapamil (Vera). After 24 h, the intracellular content of DOX was quantified fluorimetrically. Data represents the mean + SD (n=2). p=0.0378 (D) LDH-Assay to determine the cytotoxicity of DOX in combination with 6A10 or P-GP inhibitor Verapamil (Vera) on $CAXII^{high}/P\text{-}GP^{high}$ chemoresistant MDA-MB-231 cells. Cells were treated with DOX (5 µM), 6A10 (20 µg/ml), isotype control antibody (20 µg/ml) and Verapamil (75 µM). After 24 h, extracellular and intracellular LDH-activity was determined. Data presented as LDH release as percentage of total LDH-activity and represents the mean + SD (n=2). p=0.0006 (E) P-GP activity on isolated membrane fraction from MDA-MB-231 cells. Cells were incubated with 20 µg/ml 6A10 or 100 µM Verapamil for 1 h, followed by isolation of membrane fractions. P-GP activity was analyzed by measuring the ATPase activity of the enzyme by quantifying free phosphate released during ATP hydrolysis. Data are presented as mean + SD (n=2). (F) Analysis of intracellular DOX accumulation in different $CAXII^{-/low}/P\text{-}GP^{-/low}$ breast cancer cell lines. Cells were treated with 5 µM of DOX or with 20 µg/ml 6A10 antibody and DOX for 24 h. Intracellular DOX content was quantified fluorimetrically. Data represents the mean + SD (n=3). (G) LDH Assay to determine the cytotoxicity of DOX and 6A10 on different $CAXII^{-/low}/P\text{-}GP^{-/low}$ breast cancer cell lines. Cells were treated with DOX (5 µM) and 6A10 (20 µg/ml) for 24 h. Extracellular and intracellular LDH activity was determined. Data presented as LDH release as percentage of total LDH activity and represents the mean + SD (n=3).

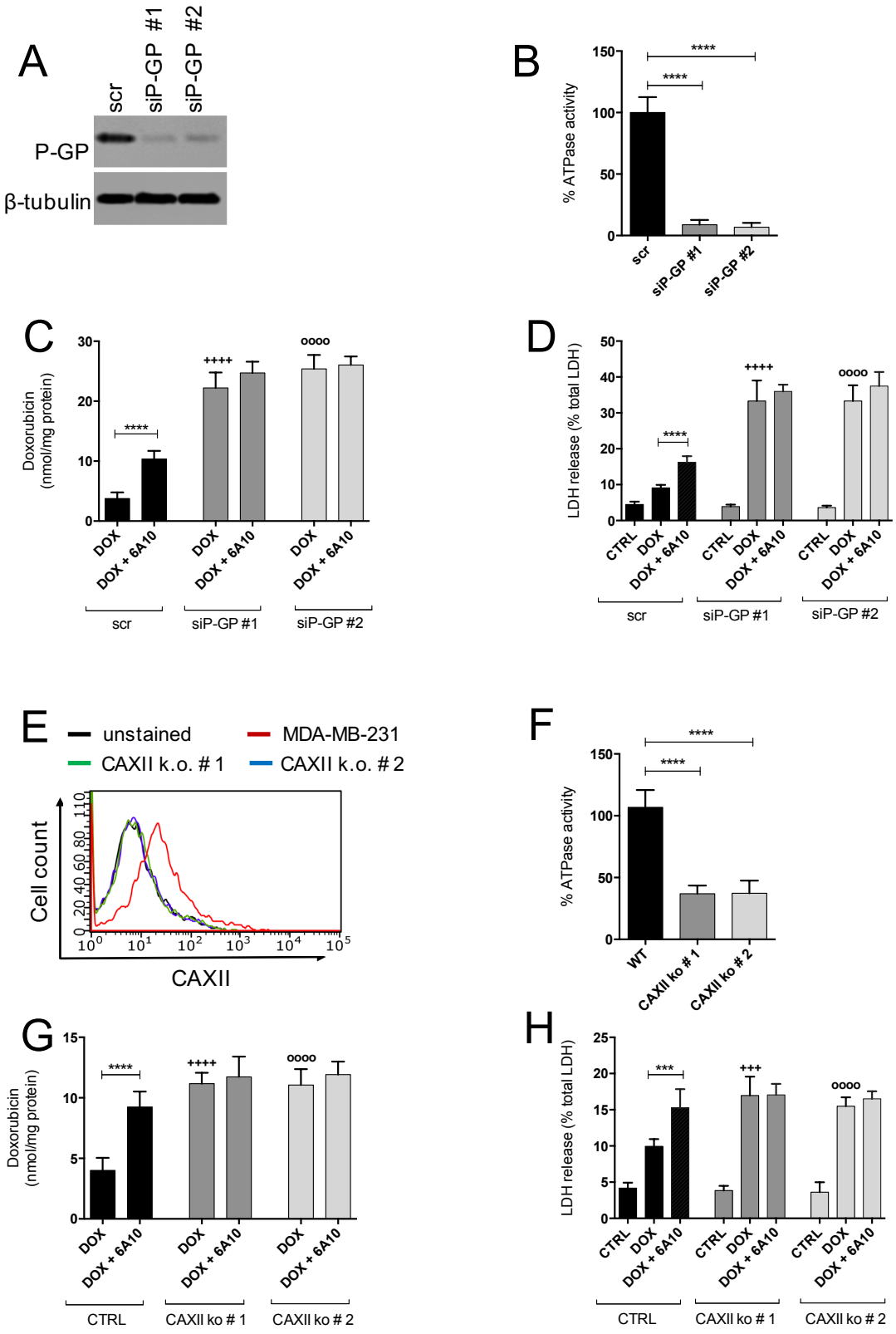

Figure 2: Knock down of P-GP and knockout of CAXII both leads to chemosensitization of resistant breast cancer cells towards DOX. (A) Expression analysis P-GP of two silenced (si)-P-GP clones by western blot using β-tubulin as a control.

60 µg protein were used per lane. P-GP was knocked out with two P-GP targeting siRNAs. Scr: non-targeting scrambled siRNA. (B) P-GP activity on isolated membrane fraction from P-GP silenced MDA-MB-231 cells. P-PG activity was analyzed by measuring the ATPase activity of the enzyme by quantifying free phosphate released during ATP hydrolysis. Data are presented as mean + SD (n=6). $p<0.0001$ (C) Intracellular accumulation of DOX in P-GP silenced MDA-MD-231 cell clones. Cells were incubated with 5 µM of DOX and or 20 µg/ml of 6A10 for 24 h, followed by the fluorimetric analysis of DOX content. Data are presented as mean + SD (n=6). DOX scr vs. DOX + 6A10 scr: $p<0.0001$, DOX scr vs. DOX siP-GP#1: $p<0.0001$, DOX scr vs. DOX siP-GP#2: $p<0.0001$ (D) Analysis of the cytotoxic effect of 6A10 and DOX on P-GP silenced MDA-MD-231 cell clones by measurement of the extracellular and intracellular LDH-activity after treatment with drugs (5 µM, 6A10 20 µg/ml) for 24 h. Data presented as LDH release as percentage of total LDH activity and represent the mean + SD (n=6). DOX scr vs. DOX + 6A10 scr: $p<0.0001$, DOX scr vs. DOX siP-GP#1: $p<0.0001$, DOX scr vs. DOX siP-GP#2: $p<0.0001$ (E) Analysis of CAXII expression by flow cytometry using 6A10 of two CAXII knocked-out (k.o). clones. Knockout of CAXII was performed by CRISPR-Cas9. (F) P-GP activity on isolated membrane fraction from CAXII k.o. MDA-MB-231 cell clones. P-GP activity was analyzed by measuring the ATPase activity of the enzyme by quantifying free phosphate released during ATP hydrolysis. Data are presented as mean + SD (n=6). $p<0.0001$ (G) Intracellular accumulation of DOX in from CAXII k.o. MDA-MB-231 cell clones. Cells were incubated with 5 µM of DOX and or 20 µg/ml of 6A10 for 24h, followed by the fluorimetric analysis of DOX content. Data are presented as mean + SD (n=6). CTRL DOX vs. CTRL DOX + 6A10: $p<0.0001$, CTRL DOX vs. CAXII k.o. #1 DOX: $p<0.0001$, CTRL DOX vs. CAXII k.o. #2 DOX: $p<0.0001$. (H) Analysis of the cytotoxic effect of 6A10 and DOX on CAXII k.o. MDA-MB-231 cell clones by measurement of the extracellular and intracellular LDH-activity after treatment with drugs (5 µM, 6A10 20 µg/ml) for 24h. Data presented as LDH-release as percentage of total LDH-activity and represents the mean + SD (n=6). CTRL DOX vs. CTRL DOX + 6A10: $p=0.0009$, CTRL DOX vs. CAXII k.o. #1 DOX: $p=0.0001$, CTRL DOX vs. CAXII k.o. #2 DOX: $p<0.0001$

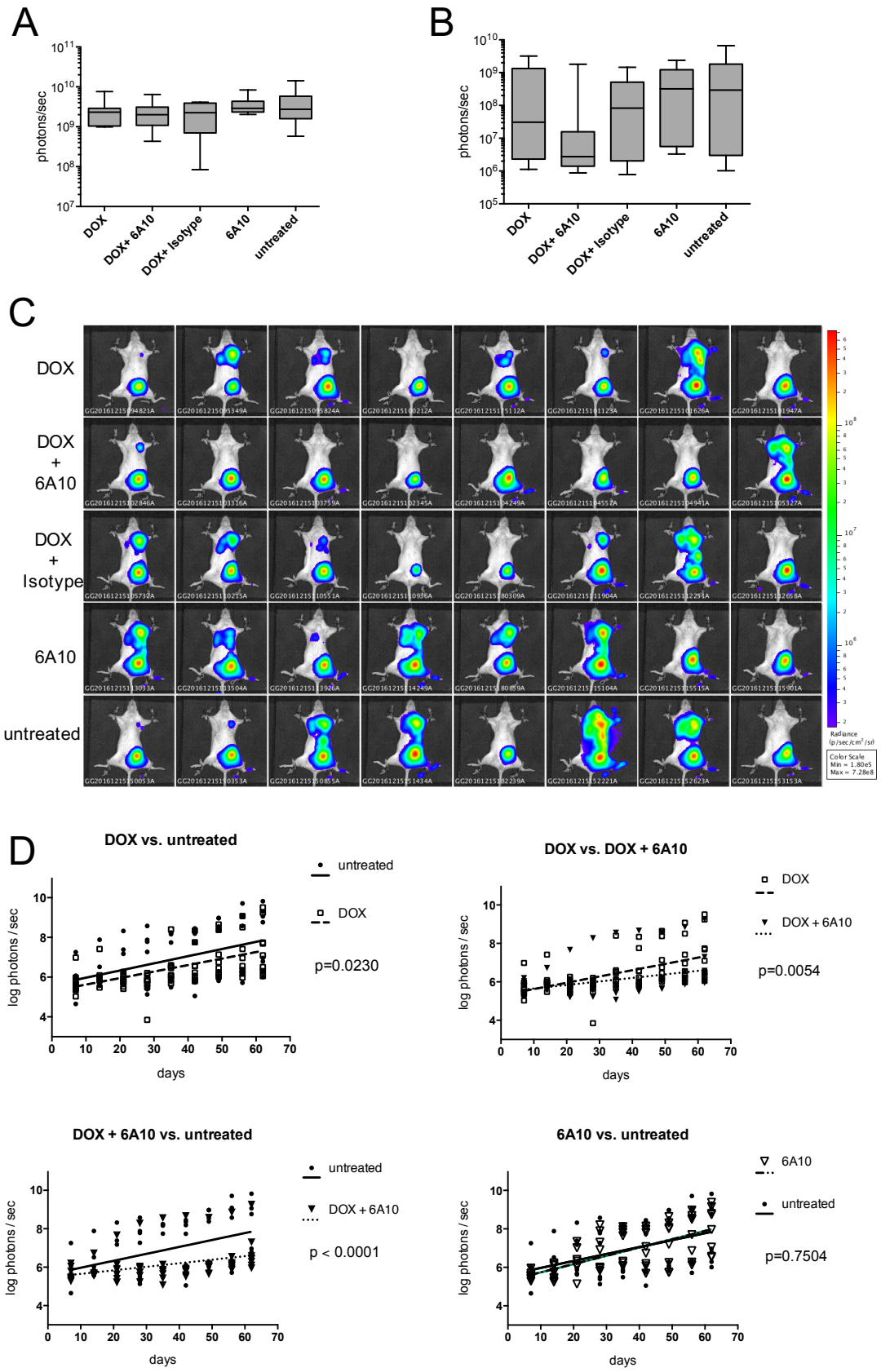

Figure 3

Figure 3: 6A10 significantly reduces the number of thoracic metastases of chemoresistant triple negative breast cancer cells in combination with DOX in an

orthotopic model. 2 x 10^6 MDA-MB-231/mCherry/fLUC cells were injected in the left inguinal mammary fad pad and tumor growth was followed by bioluminescence imaging (BLI). Treatment with 2 µg/g body weight DOX, 100 µg 6A10 or isotype control antibody twice a week was started two weeks post injection. Tumor signals were continuously measured once a week by BLI for 8 weeks. (A) Total BLI signal at week 8 of treatment (B) Thorax BLI signal at week 8 of treatment. (C) Overview of bioluminescence signals of tumor cells of all mice at end of experiment. (D) Comparison of tumor development in the thorax over time.

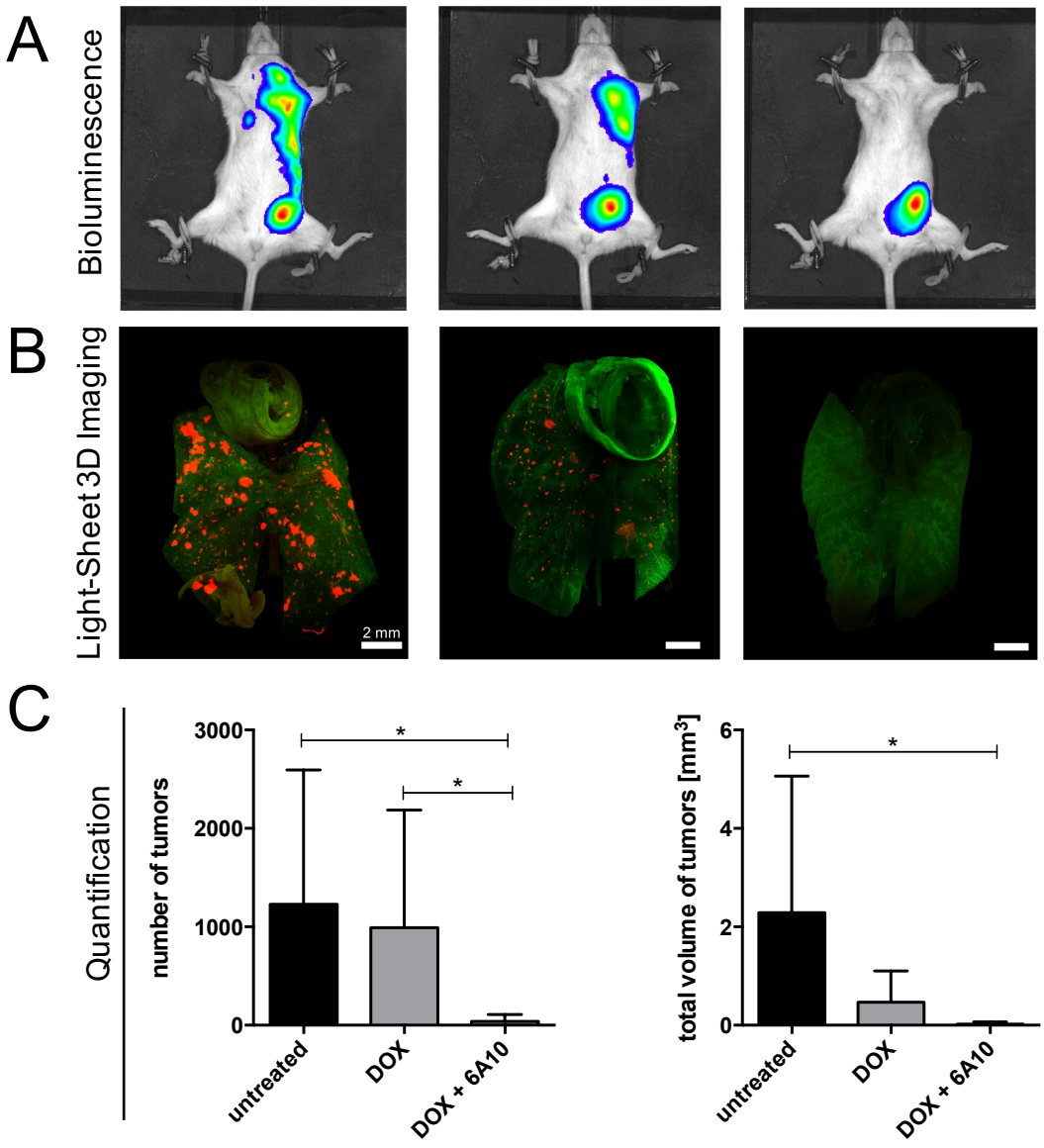

Figure 4: Analysis and quantification of lung metastases in the lungs by whole-organ imaging. (A) Bioluminescence images of untreated, DOX treated and DOX + 6A10 treated mice. **(B)** Whole organ 3D visualization of lungs from untreated, DOX and DOX + 6A10 mice obtained by light-sheet microscopy imaging. Tumor metastasis are shown in red (mCherry signal) and lung tissue are shown in green (autofluorescence signal imaged at 488 nm channel). **(C)** Analysis of tumor reduction effect of 6A10 antibody. After obtaining the light-sheet microscope images of lungs, the tumor metastases were segmented and quantified by FIJI-ImageJ software automatically. Data represents the mean + sem (n=3, 3, 4 for untreated, DOX and DOX + 6A10 groups, respectively). Number of tumors: Untreated vs. DOX + 6A10: p=0.029, DOX vs. DOX + 6A10: p=0.029. Tumor volume: Untreated vs. DOX + 6A10: p=0.029, DOX vs. DOX + 6A10: p=0.057.

Acknowledgement

This work was supported by grants from the Italian Association for Cancer Research (AIRC; IG15232 to CR), the Wilhelm Sander-Stiftung (no. 2013.009.2 to RZ) and by intramural grants from the Helmholtz Center for Environmental Health to RZ.

References

1. Loo TW, Bartlett MC, Clarke DM. The dileucine motif at the COOH terminus of human multidrug resistance P-glycoprotein is important for folding but not activity. J Biol Chem. 2005;280:2522-8.
2. Sarkadi B, Homolya L, Szakacs G, Varadi A. Human multidrug resistance ABCB and ABCG transporters: participation in a chemoimmunity defense system. Physiol Rev. 2006;86:1179-236.
3. Palmeira A, Sousa E, Vasconcelos MH, Pinto MM. Three decades of P-gp inhibitors: skimming through several generations and scaffolds. Curr Med Chem. 2012;19:1946-2025.
4. Supuran CT. Carbonic anhydrases: novel therapeutic applications for inhibitors and activators. Nat Rev Drug Discov. 2008;7:168-81.
5. Supuran CT. Inhibition of carbonic anhydrase IX as a novel anticancer mechanism. World J Clin Oncol. 2012;3:98-103.
6. Hsieh MJ, Chen KS, Chiou HL, Hsieh YS. Carbonic anhydrase XII promotes invasion and migration ability of MDA-MB-231 breast cancer cells through the p38 MAPK signaling pathway. Eur J Cell Biol. 2010;89:598-606.
7. Wykoff CC, Beasley N, Watson PH et al. Expression of the hypoxia-inducible and tumor-associated carbonic anhydrases in ductal carcinoma in situ of the breast. Am J Pathol. 2001;158:1011-9.
8. Hulikova A, Harris AL, Vaughan-Jones RD, Swietach P. Regulation of intracellular pH in cancer cell lines under normoxia and hypoxia. J Cell Physiol. 2013;228:743-52.
9. Chiche J, Ilc K, Laferriere J et al. Hypoxia-inducible carbonic anhydrase IX and XII promote tumor cell growth by counteracting acidosis through the regulation of the intracellular pH. Cancer Res. 2009;69:358-68.
10. Chiche J, Ilc K, Brahimi-Horn MC, Pouyssegur J. Membrane-bound carbonic anhydrases are key pH regulators controlling tumor growth and cell migration. Adv Enzyme Regul. 2009
11. Doyen J, Parks SK, Marcie S, Pouyssegur J, Chiche J. Knock-down of hypoxia-induced carbonic anhydrases IX and XII radiosensitizes tumor cells by increasing intracellular acidosis. Front Oncol. 2012;2:199.
12. Lounnas N, Rosilio C, Nebout M et al. Pharmacological inhibition of carbonic anhydrase XII interferes with cell proliferation and induces cell apoptosis in T-cell lymphomas. Cancer Lett. 2013
13. Morris JC, Chiche J, Grellier C et al. Targeting hypoxic tumor cell viability with carbohydrate-based carbonic anhydrase IX and XII inhibitors. J Med Chem. 2011;54:6905-18.
14. Battke C, Kremmer E, Mysliwietz J et al. Generation and characterization of the first inhibitory antibody targeting tumour-associated carbonic anhydrase XII. Cancer Immunol Immunother. 2011;60:649-58.
15. Gondi G, Mysliwietz J, Hulikova A et al. Antitumor efficacy of a monoclonal antibody that inhibits the activity of cancer-associated carbonic anhydrase XII. Cancer Res. 2013;73:6494-503.
16. Kopecka J, Campia I, Jacobs A et al. Carbonic anhydrase XII is a new therapeutic target to overcome chemoresistance in cancer cells. Oncotarget. 2015;6:6776-93.
17. Iorns E, Drews-Elger K, Ward TM et al. A new mouse model for the study of human breast cancer metastasis. PLoS One. 2012;7:e47995.
18. Terziyska N, Castro Alves C, Groiss V et al. In vivo imaging enables high resolution preclinical trials on patients' leukemia cells growing in mice. PLoS One. 2012;7:e52798.
19. Pan C, Cai R, Quacquarelli FP et al. Shrinkage-mediated imaging of entire organs and organisms using uDISCO. Nat Methods. 2016;13:859-67.
20. Steeg PS, Theodorescu D. Metastasis: a therapeutic target for cancer. Nat Clin Pract

Oncol. 2008;5:206-19.
21. Amin ML. P-glycoprotein Inhibition for Optimal Drug Delivery. Drug Target Insights. 2013;7:27-34.
22. Thomas H, Coley HM. Overcoming multidrug resistance in cancer: an update on the clinical strategy of inhibiting p-glycoprotein. Cancer Control. 2003;10:159-65.
23. Juweid M, Neumann R, Paik C et al. Micropharmacology of monoclonal antibodies in solid tumors: direct experimental evidence for a binding site barrier. Cancer Res. 1992;52:5144-53.
24. Thurber GM, Zajic SC, Wittrup KD. Theoretic criteria for antibody penetration into solid tumors and micrometastases. J Nucl Med. 2007;48:995-9.
25. Ertürk A, Mauch CP, Hellal F et al. Three-dimensional imaging of the unsectioned adult spinal cord to assess axon regeneration and glial responses after injury. Nat Med. 2011;18:166-71.
26. Ertürk A, Becker K, Jährling N et al. Three-dimensional imaging of solvent-cleared organs using 3DISCO. Nat Protoc. 2012;7:1983-95.
27. Kopecka J, Rankin GM, Salaroglio IC, Poulsen SA, Riganti C. P-glycoprotein-mediated chemoresistance is reversed by carbonic anhydrase XII inhibitors. Oncotarget. 2016;7:85861-75.
28. Riganti C, Voena C, Kopecka J et al. Liposome-encapsulated doxorubicin reverses drug resistance by inhibiting P-glycoprotein in human cancer cells. Mol Pharm. 2011;8:683-700.
29. Vick B, Rothenberg M, Sandhöfer N et al. An advanced preclinical mouse model for acute myeloid leukemia using patients' cells of various genetic subgroups and in vivo bioluminescence imaging. PLoS One. 2015;10:e0120925.

Supplementary Data

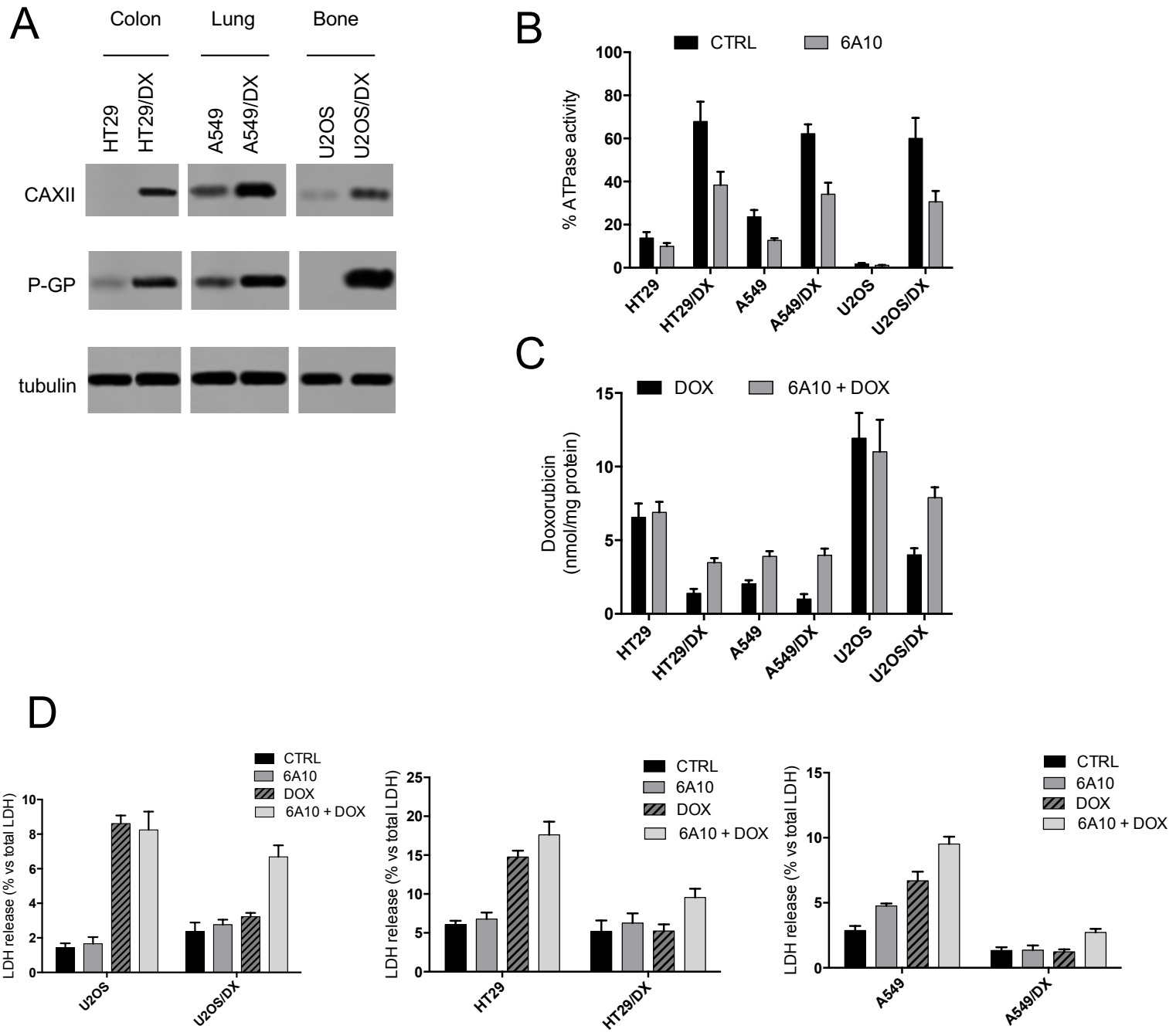

Figure S1: 6A10 increases intracellular Doxorubicin accumulation and cytotoxicity in CAXII$^+$/P-GP$^+$ cells of different origin. (A) Western Blot analysis of P-GP expression in human colon cancer HT29 and in doxoroubicin-resistant counterpart HT29/DX, in lung cancer A549 and in doxoroubicin-resistant counterpart A549/DX, in osteosarcoma U-2OS and in doxoroubicin-resistant counterpart U-2OS/DX. 60 µg per lane were analyzed. β-Tubulin was used as a control for equal protein loading. **(B)** P-GP activity on isolated membrane fractions. Cells were incubated in the absence (CTRL) or presence of 20 µg/ml 6A10 for 1h, followed by isolation of membrane fractions. P-GP activity was analyzed by measuring the ATPase activity of the enzyme by quantifying free phosphate released during ATP hydrolysis. Data is presented as mean + SD (n=2). **(C)** Intracellular accumulation of doxorubicin (DOX). Cells were incubated with 5 µM of DOX and or 20 µg/ml of 6A10 for 24h, followed by the fluorimetric analysis of DOX content. Data is presented as mean + SD (n=6). **(D)** Analysis of the cytotoxic effect of 6A10 and DOX by measurement of the extracellular and intracellular LDH activity after treatment with drugs (5 µM, 6A10 20 µg/ml) for 24h. Data presented as LDH release as percentage of total LDH activity and represents the mean + SD (n=6).

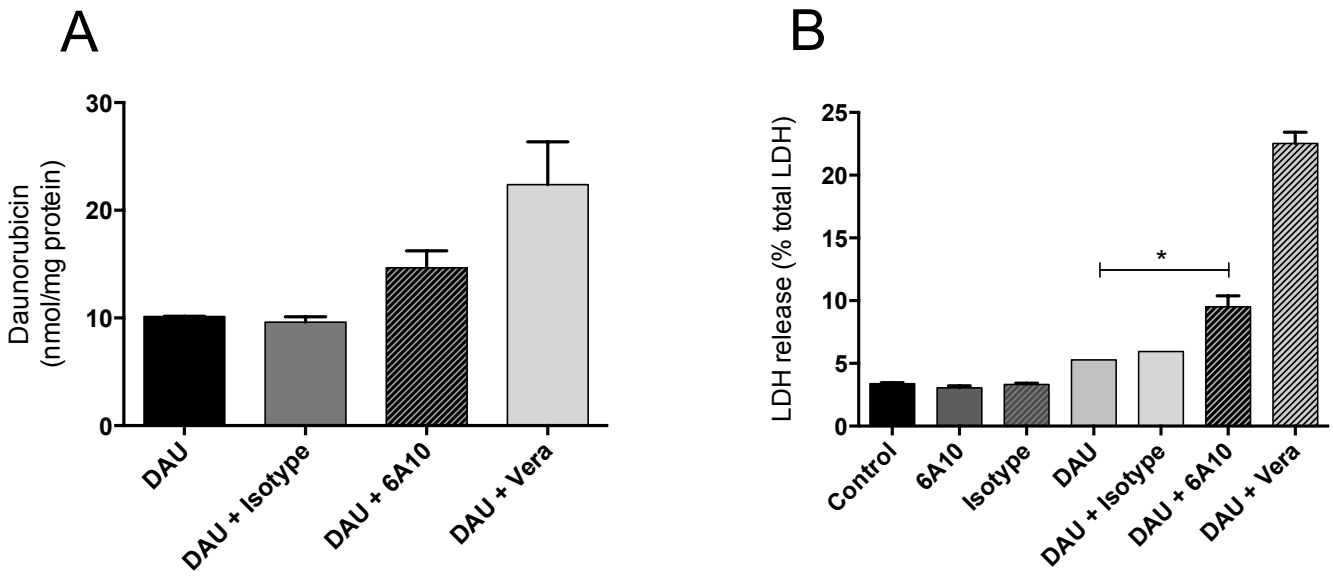

Figure S2: 6A10 also increases intracellular accumulation of anthracycline daunorubicin (DAU) as well as cytotoxicity of CAXII$^+$/P-GP$^+$ chemoresistant triple negative MDA-MB-231 breast cancer cells. (A) Analysis of intracellular DAU accumulation. Cells were treated with 5 µM of DAU in combination with 20 µg/ml 6A10 antibody, an Isotype control antibody or 75 µM P-GP inhibitor Verapamil for 24h. Intracellular content of DAU was quantified fluorimetrically. Data represents the mean + SD (n=2). **(B)** LDH-Assay to determine the cytotoxicity of DAU in combination with 6A10 or P-GP inhibitor Verapamil. Cells were treated with DAU (5 µM), 6A10 (20 µg/ml), Isotype control antibody (20 µg/ml) and Verapamil (75 µM) for 24h. Extracellular and intracellular LDH activity was determined. Data presented as LDH release as percentage of total LDH activity and represents the mean + SD (n=2). p=0.0211

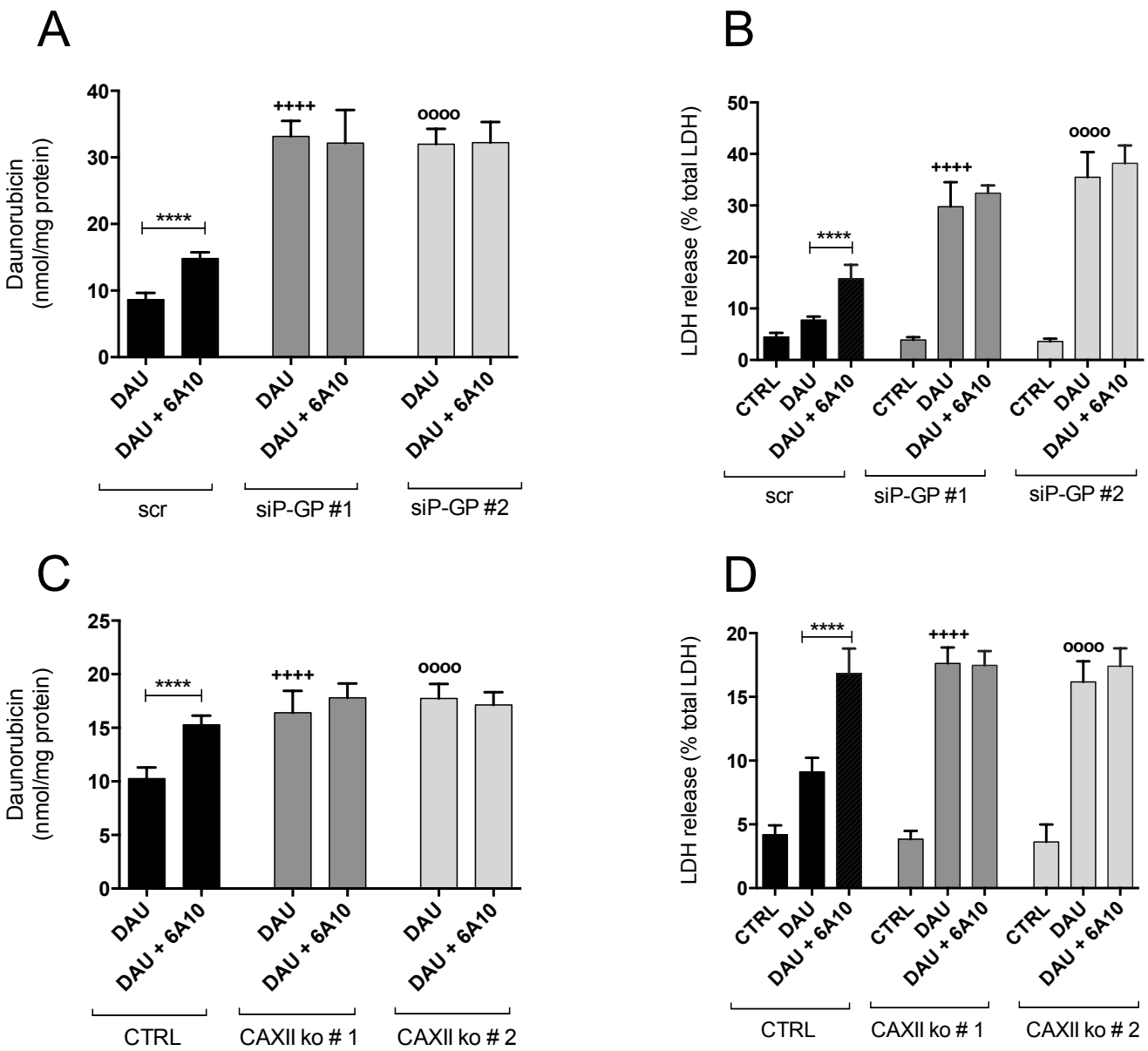

Figure S3: Knock down of P-GP and knockout of CAXII both leads to chemosensitation of resistant breast cancer cells towards Daunorubicin (DAU). P-GP was knocked out by two P-GP targeting siRNA. Scr: not-targeting scarmbled siRNA. **(A)** Intracellular accumulation of DAU in P-GP silenced MDA-MD-231 cell clones. Cells were incubated with 5 µM of DAU and or 20 µg/ml of 6A10 for 24h, followed by the fluorimetric analysis of DAU content. Data is presented as mean + SD (n=6). DAU scr vs. DAU + 6A10 scr: $p<0.0001$, DAU scr vs. DAU siP-GP#1: $p<0.0001$, DAU scr vs. DAU siP-GP#2: $p<0.0001$. **(B)** Analysis of the cytotoxic effect of 6A10 and DAU on P-GP silenced MDA-MD-231 cell clones by measurement of the extracellular and intracellular LDH activity after treatment with drugs (5 µM, 6A10 20 µg/ml) for 24h. Data presented as LDH release as percentage of total LDH activity and represents the mean + SD (n=6). DAU scr vs. DAU + 6A10 scr: $p<0.0001$, DAU scr vs. DAU siP-GP#1: $p<0.0001$, DAU scr vs. DAU siP-GP#2: $p<0.0001$. **(C)** Intracellular accumulation of DAU in from CAXII ko MDA-MB-231 cell clones. Knock-out of CAXII was performed by CRISPR-Cas9. Cells were incubated with 5 µM of DAU and or 20 µg/ml of 6A10 for 24h, followed by the fluorometric analysis of DAU content. Data is presented as mean + SD (n=6). CTRL DAU vs. CTRL DAU + 6A10: $p<0.0001$, CTRL DAU vs. CAXII ko #1 DAU: $p<0.0001$, CTRL DAU vs. CAXII ko #2 DAU: $p<0.0001$. **(D)** Analysis of the cytotoxic effect of 6A10 and DAU on CAXII ko MDA-MB-231 cell clones by measurement of the extracellular and intracellular LDH activity after treatment with drugs (5 µM, 6A10 20 µg/ml) for 24h. Data presented as LDH release as percentage of total LDH activity and represents the mean + SD (n=6). CTRL DAU vs. CTRL DAU + 6A10: $p<0.0001$, CTRL DAU vs. CAXII ko #1 DAU: $p<0.0001$, CTRL DAU vs. CAXII ko #2 DAU: $p<0.0001$.

Supplementary Data

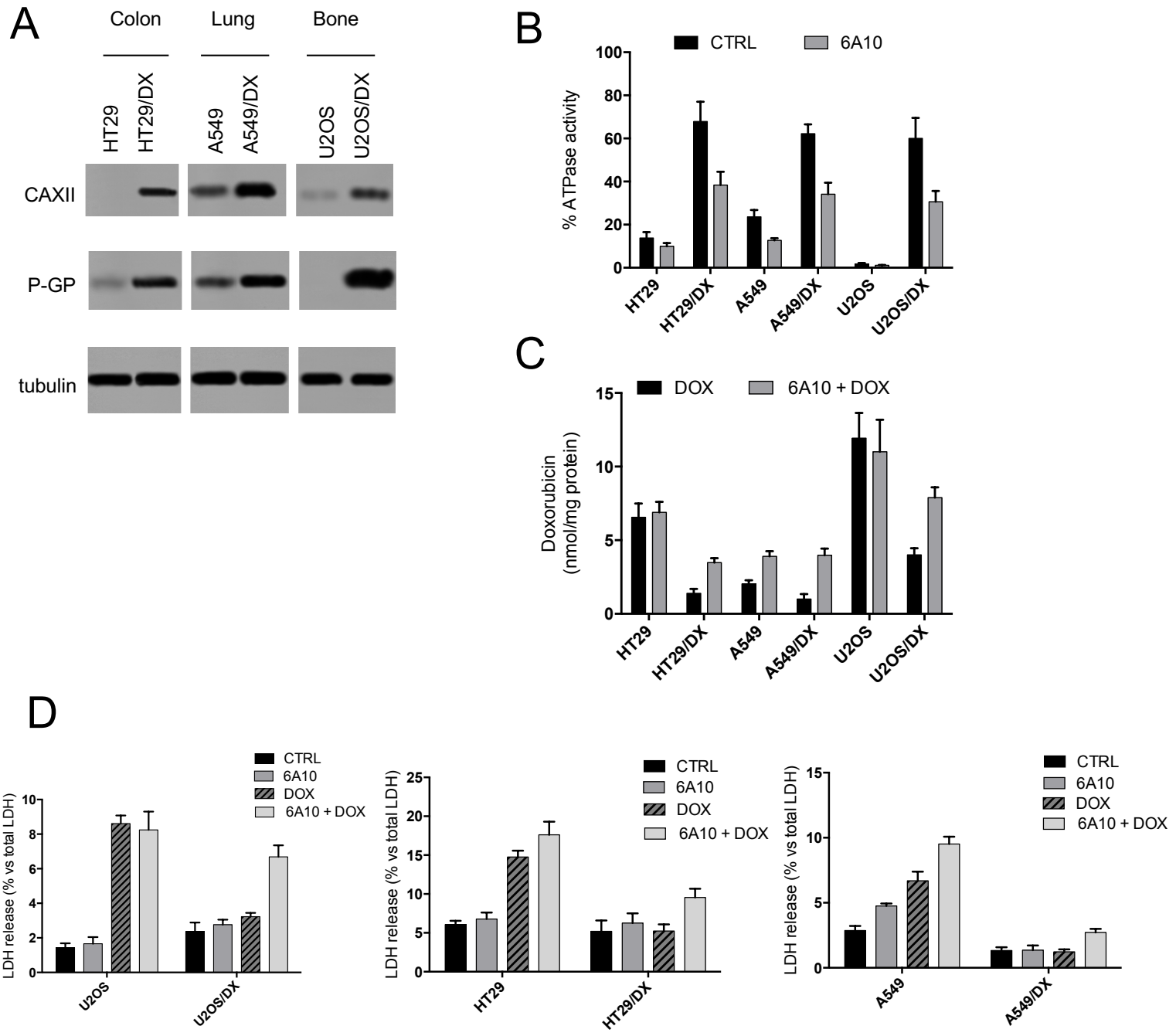

Figure S1: 6A10 increases intracellular Doxorubicin accumulation and cytotoxicity in CAXII$^+$/P-GP$^+$ cells of different origin. (A) Western Blot analysis of P-GP expression in human colon cancer HT29 and in doxoroubicin-resistant counterpart HT29/DX, in lung cancer A549 and in doxoroubicin-resistant counterpart A549/DX, in osteosarcoma U-2OS and in doxoroubicin-resistant counterpart U-2OS/DX. 60 µg per lane were analyzed. β-Tubulin was used as a control for equal protein loading. **(B)** P-GP activity on isolated membrane fractions. Cells were incubated in the absence (CTRL) or presence of 20 µg/ml 6A10 for 1h, followed by isolation of membrane fractions. P-GP activity was analyzed by measuring the ATPase activity of the enzyme by quantifying free phosphate released during ATP hydrolysis. Data is presented as mean + SD (n=2). **(C)** Intracellular accumulation of doxorubicin (DOX). Cells were incubated with 5 µM of DOX and or 20 µg/ml of 6A10 for 24h, followed by the fluorimetric analysis of DOX content. Data is presented as mean + SD (n=6). **(D)** Analysis of the cytotoxic effect of 6A10 and DOX by measurement of the extracellular and intracellular LDH activity after treatment with drugs (5 µM, 6A10 20 µg/ml) for 24h. Data presented as LDH release as percentage of total LDH activity and represents the mean + SD (n=6).

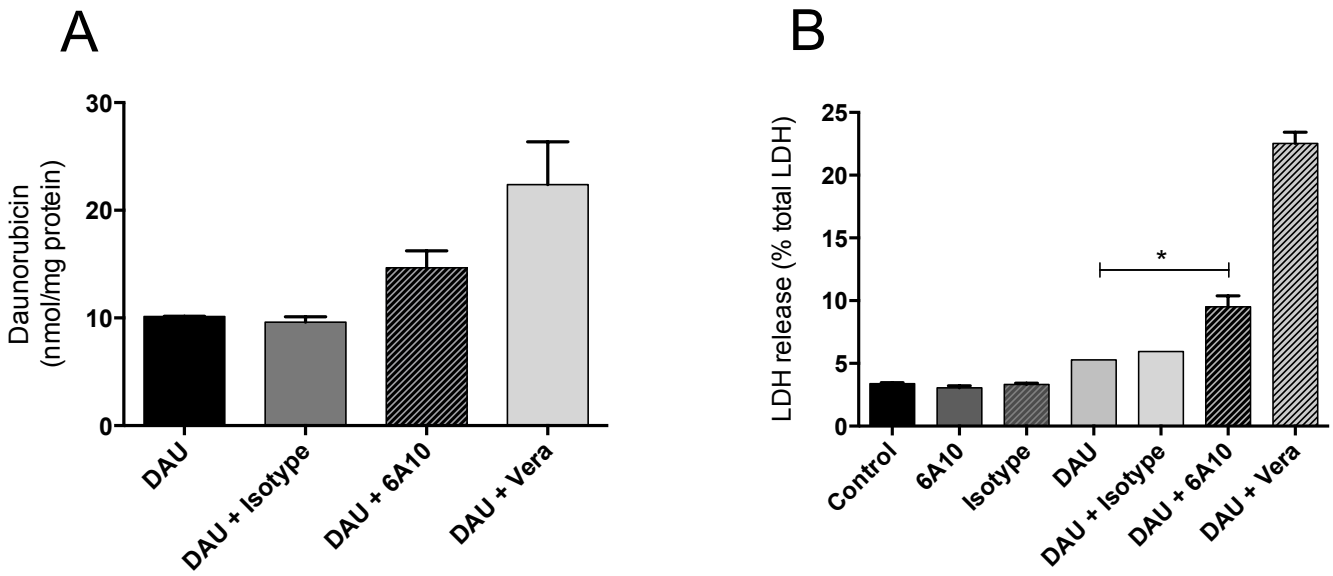

Figure S2: 6A10 also increases intracellular accumulation of anthracycline daunorubicin (DAU) as well as cytotoxicity of CAXII$^+$/P-GP$^+$ chemoresistant triple negative MDA-MB-231 breast cancer cells. (A) Analysis of intracellular DAU accumulation. Cells were treated with 5 µM of DAU in combination with 20 µg/ml 6A10 antibody, an Isotype control antibody or 75 µM P-GP inhibitor Verapamil for 24h. Intracellular content of DAU was quantified fluorimetrically. Data represents the mean + SD (n=2). **(B)** LDH-Assay to determine the cytotoxicity of DAU in combination with 6A10 or P-GP inhibitor Verapamil. Cells were treated with DAU (5 µM), 6A10 (20 µg/ml), Isotype control antibody (20 µg/ml) and Verapamil (75 µM) for 24h. Extracellular and intracellular LDH activity was determined. Data presented as LDH release as percentage of total LDH activity and represents the mean + SD (n=2). p=0.0211

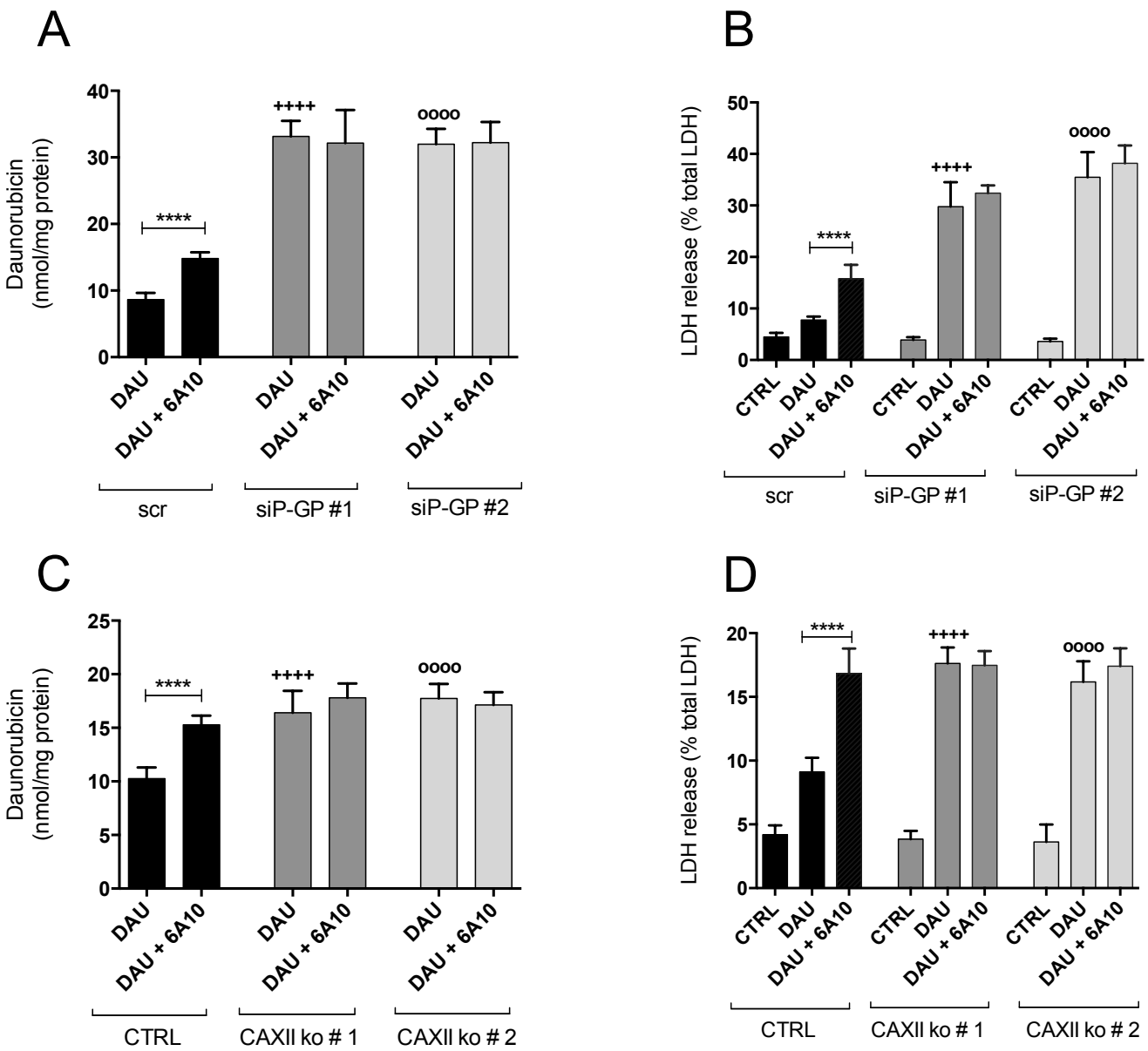

Figure S3: Knock down of P-GP and knockout of CAXII both leads to chemosensitation of resistant breast cancer cells towards Daunorubicin (DAU). P-GP was knocked out by two P-GP targeting siRNA. Scr: not-targeting scarmbled siRNA. **(A)** Intracellular accumulation of DAU in P-GP silenced MDA-MD-231 cell clones. Cells were incubated with 5 µM of DAU and or 20 µg/ml of 6A10 for 24h, followed by the fluorimetric analysis of DAU content. Data is presented as mean + SD (n=6). DAU scr vs. DAU + 6A10 scr: $p<0.0001$, DAU scr vs. DAU siP-GP#1: $p<0.0001$, DAU scr vs. DAU siP-GP#2: $p<0.0001$. **(B)** Analysis of the cytotoxic effect of 6A10 and DAU on P-GP silenced MDA-MD-231 cell clones by measurement of the extracellular and intracellular LDH activity after treatment with drugs (5 µM, 6A10 20 µg/ml) for 24h. Data presented as LDH release as percentage of total LDH activity and represents the mean + SD (n=6). DAU scr vs. DAU + 6A10 scr: $p<0.0001$, DAU scr vs. DAU siP-GP#1: $p<0.0001$, DAU scr vs. DAU siP-GP#2: $p<0.0001$. **(C)** Intracellular accumulation of DAU in from CAXII ko MDA-MB-231 cell clones. Knock-out of CAXII was performed by CRISPR-Cas9. Cells were incubated with 5 µM of DAU and or 20 µg/ml of 6A10 for 24h, followed by the fluorometric analysis of DAU content. Data is presented as mean + SD (n=6). CTRL DAU vs. CTRL DAU + 6A10: $p<0.0001$, CTRL DAU vs. CAXII ko #1 DAU: $p<0.0001$, CTRL DAU vs. CAXII ko #2 DAU: $p<0.0001$. **(D)** Analysis of the cytotoxic effect of 6A10 and DAU on CAXII ko MDA-MB-231 cell clones by measurement of the extracellular and intracellular LDH activity after treatment with drugs (5 µM, 6A10 20 µg/ml) for 24h. Data presented as LDH release as percentage of total LDH activity and represents the mean + SD (n=6). CTRL DAU vs. CTRL DAU + 6A10: $p<0.0001$, CTRL DAU vs. CAXII ko #1 DAU: $p<0.0001$, CTRL DAU vs. CAXII ko #2 DAU: $p<0.0001$.